MOLECULAR DOCKING AND MOLECULAR DYNAMICS STUDY OF ALCOHOLIC COMPOUNDS AS MYCOBACTERICIDAL AGENTS USING INHA, MABA AND PANK AS RECEPTORS

Gita Syahputra[1*], Arwansyah[2], Wien Kusharyoto[1]

[1]Laboratory for Applied Genetic Engineering and Protein Design
Research Center for Biotechnology-LIPI, Bogor, Indonesia 16911
[2] Department of Chemistry, Cokroaminoto University, Palopo, Indonesia 91911

Abstract

Tuberculosis (TB) infection is one of the primary infectious diseases in many developing countries; even there are minor cases in some developed countries. TB infection spread through the air and is more probable when using improper disinfectant on medical and laboratory equipment which related to TB research. The appropriate disinfectants which are commonly used in laboratory equipment can reduce the risk of transmission of TB disease. Alcoholic compounds are one of the common disinfectants with a broad spectrum activity towards microbes, viruses, and fungus. We employed molecular docking and molecular dynamics simulation to support virtual screening and ligand-receptor complex binding observation in searching for an appropriate mycobactericidal agent. Based on the analysis of molecular docking and molecular dynamics, pentadecanol has potency as a mycobactericidal agent with PanK as its specific receptor. The Gibbs free energy (ΔG) for the interaction of pentadecanol with PanK has been found to be -5.5 kcal/mol. Molecular dynamics analysis at 300K and 1 atm for 5 ns showed a little change in the confirmation of the binding site, while pentadecanol was still being bound by its binding site on PanK.

Keywords: alcoholic compounds, disinfectant, molecular docking, molecular dynamics, mycobactericidal

---

[*]Corresponding author:
Research Center for Biotechnology - LIPI, Jl. Raya Bogor Km. 46, Cibinong 16911, Indonesia
Tel. +62-21-8754587, Fax. +62-21-87754588
E-mail. gitasyahputra@gmail.com/gita003@lipi.go.id

Introduction

Based on data collected from the World Health Organization (WHO) in 2018, tuberculosis (TB) still belongs to the top ten diseases causing deaths in the world. In 2016, WHO reported that about 10.4 million people contracted TB, with 1.7 million people died (including 400 thousand inhabitants who also contracted the HIV). TB infection by *Mycobacterium tuberculosis* was further improved on the basis of reports of several cases of multidrug resistance and resistant (MDR) antibiotic that exists today. TB infection has been the major infectious diseases in many developing countries; even there are minority cases in the developed countries like Japan, Australia, the USA, and Germany (Kato *et al*., 2016; Toms *et al*., 2015; Stewart *et al*., 2018; Hauer *et al*., 2018).

Some public places have been reported to be the sites of infection; among them are hospitals (Ehrenkranz and Kicklighter, 1972), jail (Mohle-Boetani *et al*., 2002), an orphanage (Curtis *et al*., 2000). The causal factor of TB infection includes the abortive attempt of the national vaccination program, inadequate of health facilities, less effective antituberculosis medications, and resilience of the human body against pathogens (Bloom *et al*., 1992). Report of the year 2016 at a health facility that handles TB disease in Ikeja, Lagos City, Nigeria found a managerial weakness in Tuberculosis Infection Control (TBIC) (Kuyinu *et al*., 2016). Research in Lima, Peru has been uncovering the existence of potential TB infection at the

DOI: http://dx.doi.org/10.14203/ann.bogor.2018.v22.n2.101-115

Emergency Department (ED) (Escombe *et al*., 2010). In 2010, a school in Southern India reported the presence of TB infection on a nurse candidate (Christopher *et al*., 2010). The appropriate disinfectants which commonly used in laboratory equipment can reduce the risk of transmission of TB disease occur (Best *et al*., 1990; Rutala *et al*., 1991; Dauendorffer *et al*., 1999).

The TB infection spreads through the air and is more probable when using improper disinfectant on medical and laboratory equipment which related to TB research (Spach *et al*., 1993). Disinfectants are the chemical agents that can kill microorganisms, but not for bacterial spores (Schroeder *et al*., 2002). The study was essential in investigating the most effective disinfectants as a mycobactericidal agent through the reaction of some mycobactericidal compounds against *M. tuberculosis*. Uniquely, the cell wall structure of *M. tuberculosis* has a hydrophobic characteristic and more resistant to biocide compared to other bacteria, therefore the bacteria capable of surviving longer in a specific environment (van Klingeren *et al*., 1987, Breenan, 2003, Russell, 1999, Kunzand Gundermann, 1982).

Alcoholic compounds and its derivatives have been demonstrated to having antimycobacterial activity (Junior *et al*., 2009; Rugutt and Rugutt, 2011; Falkinham *et al*., 2012). The antimycobacterial activity of alcoholic compounds influenced by the amount of carbon (C) chain, polarity, double and triple bond in the alcohol structure (Kabelitz N *et al*., 2003). A previous study reported that alcohols with 7-10 C-atoms have the potential as antimycobacterial, while C_{10} (1-decanol) has the best capabilities in the inhibition of *M.bovis* and *M. tuberculosis* (Mukherjee *et al*., 2012). However, there were only a few studies about the action of alcohols as a disinfectant. Generally, alcohol is known to act as the destroyer of the cell membranes and denaturation of proteins that influence the metabolism and cell lysis (Larson *et al*.,1994; Morton, 1983; Sykes, 1970).

Some of the enzymes involved in the biosynthesis of. *tuberculosis* cell wall and become an interesting target in the drug design of antituberculosis compounds (Jackson *et al*., 2013). The function of enoyl-acyl carrier protein reductase (InhA) is to catalyze the reduction process of 2-trans-enoyl carbon chains with at least 12 C chain. The enzyme is responsible for the ending process of each elongation of two-carbon in fatty acids biosynthesis. InhA involves in the production of long-chain fatty acid and mycolic acid, which makes it an exciting target in inhibitor design to inhibit the biosynthesis of fatty acid chains on *M. tuberculosis* cell walls (Marrakchi H et al., 2000; Dessen et al.,1995; Banerjee et al., 1994). On the other hand, pantothenate kinases (PanK) is a biocatalyst which capable of regulating the biosynthesis of Cofactor A (CoA). CoA is necessary for enzymatic reactions as a carrier of acyl group in the biosynthesis of oxidative tricarboxylic and metabolism of fatty acids (Leonardi *et al*., 2005; Jackowski and Rock, 1981; Zhou *et al*., 2001; Rock *et al*., 2002). The fatty acids type II system (FAS II) elongation is catalyzed by β-ketoacyl-ACP reductase (MabA). The enzyme is responsible for the production of long-chain fatty acids and their derivatives that become the key for the formation of mycolic acid, the main content in the *M. tuberculosis* cell walls (Marrakchi *et al*., 2000, 2002; Takayama *et al*., 2005).

Discovery and drug design are the processes which involve many scientific disciplines such as medicinal chemistry, pharmacology, biochemistry, and computational biology. Previously, researchers conducted trial-and-error processes to search for the inhibitor for drug development, which took time and money. Currently, the computational methods support the drug design process more effectively (Schneider *et al*., 2005; Kapetanovi, 2008). The virtual screening process involves the computer-aided drug design and development method (CADDD). Virtual screening methods employ the molecular docking simulation for describing the orientation of small molecules binding to protein target based on the calculation of activity and affinity values. The CADDD exploit the dynamic molecular simulations for predicting the stability of ligand complexes with proteins. (Alonso *et al*., 2006; Zhao and Caflisch, 2014; Tambunan *et al*., 2017).

Determination of appropriate disinfectant is essential for the control the infectious diseases from spreading in public (Hatipoglu *et al*., 2016). Hence, we employed molecular docking and molecular dynamics simulations to investigate the potential of alcoholic compounds (C_1-C_{15}) as an appropriate

DOI: http://dx.doi.org/10.14203/ann.bogor.2018.v22.n2.101-115

disinfectant to eradicate *M. tuberculosis* growth. The purpose of this study is (1)to calculate the binding energy by molecular docking simulation (2) to investigate the stability of potential ligand-receptor complex binding by molecular dynamics simulation. The research results have a preliminary study as a reference to *in vitro* and *in vivo* study.

Materials and Methods

Software and hardware.

The computational visualization and analysis of molecular docking and molecular dynamics results were conducted using PyMol (https://pymol.org/2/), Visual Molecular Dynamics (VMD) (http://www.ks.uiuc.edu/Research/vmd/), and Ligplot Plus (https://www.ebi.ac.uk/thornton-srv/software/-LigPlus/). For this study, we used ASUS workstation machine running on Intel ® Core™ i3 CPU processor with 2 GB RAM and 500 GB hard disk using Windows as the operating system.

Ligand preparation.

All chemical structures; alcoholic compounds (C_1-C_{15}), isoniazid, and triclosan were selected for the docking analysis, and the structure was retrieved from the PubChem chemical structure database (https://pubchem.ncbi.nlm.nih.gov/) (Wang *et al*., 2009). Isoniazid is one of the drugs for TB medicine, and triclosan is the common ingredient in disinfectant products. Isoniazid and triclosan were used in comparing the mycobactericidal activity with the alcoholic compounds used in this study. All of the chemical structures were saved in PDB format.

Receptor preparation.

The three-dimensional (3D)-structures of the target receptors or enzymes (InhA, MabA, and PanK) were obtained from Protein Data Bank (PDB) (https://www.wwpdb.org/) (Berman *et al*., 2002). The following crystal structures were used for this study: for InhA (PDB ID: 2B37), for MabA (PDB ID: 1UZN), for PanK (PDB ID: 3AF3) (Shilpi *et al*., 2015)

Based on the previous study, the binding site residues for InhA, MabA, and PanK were identified (Table 1) (Rozwarski *et al*., 1999; Marrakchi *et al*., 2000; Shilpi *et al*., 2015).

Table 1. Binding sites selected for the receptors

Protein Name	Binding site residues
InhA	Met103, Phe149, Met155, Tyr158, Met161, Ala198, Met199, Ala201, Ile202, Leu207, Ile216, Leu218, Thr196
MabA	Gly22, Asn24, Ile27, Arg47, Asp61, Val62, Gly90, Asn88, Ser140, Ile138, Gly139, Tyr153, Ile186, Lys157.
PanK	Gly97, Ser98, Val99, Ala100, Val101, Gly102, Lys103, Ser104, His179, Tyr235, Arg238, Met242, Asn277

Ligand-receptor docking.

Study for molecular docking was performed using the AutoDock Vina 4.2 program (http://vina.scripps.edu/). Docking preparation steps for ligand and receptor were performed using the AutoDock Tools (ADT) 1.5.4 program. The receptor preparation was focused on adding all hydrogen atoms into the receptor and grid box parameters. The grid box for InhA (x= 12.832, y= 16.388, z= 6.306), MabA (x= 3.562, y= 17.424, z= 11.951), and PanK (x= -40.278, y= 34.674, z= -5.52), with 1 Å spacing (Shilpi *et al*., 2015). The ligand preparation was focused on adding non-polar hydrogen and assigning torsion degrees. The Lamarckian Genetic Algorithm (LGA) was used during the docking process to explore the best conformational space for the ligand. LGA was applied to model the interaction pattern between receptors and the ligand (Morris *et al*., 2009). The molecular docking was supported by virtual screening based on the minimum Gibbs free energy (ΔG). The negative value of Gibbs free energy (ΔG) implies that the ligand has a potency to inhibit the receptor pathway.

Molecular dynamics.

The general Amber force field (GAFF) was used to determine the force field of the ligand molecule, and the AMBER14 force field was used for the protein molecule. The crystal structure of protein and ligand in the system were added by TIP3P- water molecules in 138.598 x 80.056 x 148.124 Ā periodic box; then the system was neutralized with one Na^+ ion. The long-range electrostatic interactions

DOI: http://dx.doi.org/10.14203/ann.bogor.2018.v22.n2.101-115

were calculated by Particle Mesh Ewald (PME) method and the hydrogen bond was constrained with the SHAKE Algorithm. The temperature and pressure coupling were controlled at 300 K and 1 atm using Langevin thermostat and isotropic position scaling algorithm with the time step of 2.0 fs. After energy minimization with a constraint on the protein and ligand, we performed energy minimization with no constraint. The system was equilibrated by gradually increasing the temperature from 0 to 300 K for 60 ps by using an *NVT* ensemble. After the system reached the equilibration, *NPT* ensemble was performed without harmonic position constraint for 5 ns. The simulation was performed using AmberTools 16 packages (Salomon-Ferrer, R*et al*., 2013). The analysis of the trajectories of MD simulation was conducted using CPPTRAJ tools. The RMSD value of the complex is represented as:

$$RMSD(t_1, t_2) = [\frac{1}{M} \sum_{i=1}^{N} m_i \| r_i(t_1) - r_i(t_2) \|^2]^{1/2},$$

where *N* is the total number of an atom, m_i is the mass of atoms and $r_i(t_1)$is the position of backbone atoms of PanKenzyme and C; N; O; H atoms of ligand molecule at the time t_1, and$r_i(t_2)$ is the position of atoms of PanKenzyme from the X-ray structure and the initial position of Pentadecanol obtained from docking simulation, respectively (Roe& Cheatham, 2013)

Results

Gibbs free energy (ΔG).

Molecular docking was performed on alcoholic compounds (C_1-C_{15}) to InhA, MabA, and PanK receptors. Molecular docking is profitable to virtual screening the inhibitory potential of alcoholic compounds toward receptors. The potency of alcohols was indicated by Gibbs free energy (ΔG) from molecular docking results. The more negative Gibbs free energy (ΔG) values indicate more stable and stronger binding energy on ligand and receptor.

Table 2 shows Gibbs free energy (ΔG) obtained from Lamarckian Genetic Algorithm (LGA) calculation on AutoDock Vina. The values of Gibbs free energy (ΔG) revealed that the alcoholic compounds had more potential in PanK inhibition, which was indicated by the stronger binding energy of alcoholic compounds with PanK when compared to the bonding energy of alcoholic compoundstowardsMabA and InhA. The value (ΔG) of the methanol bond with each receptor, reported binding energy of methanol-PanK more negative (ΔG: -2.4 kcal/mol), compared with the binding energy of methanol-InhA (ΔG: -1.8 kcal/mol)and the energy binding of methanol-MabA (ΔG: -2.0 kcal/mol).

Table 2. Gibbs free energy (ΔG) (kcal/mol) for molecular docking of ligand-receptor

Ligand \ Receptor	InhA	MabA	PanK
Methanol (C_1)	-1.8	-2.0	-2.4
Ethanol (C_2)	-2.3	-2.7	-2.8
Propanol (C_3)	-3.4	-3.0	-3.1
Butanol (C_4)	-3.0	-3.2	-3.3
Pentanol (C_5)	-3.3	-3.4	-3.5
Hexanol (C_6)	-3.6	-3.7	-3.9
Heptanol (C_7)	-3.9	-3.7	-4.4
Octanol (C_8)	-4.2	-3.9	-4.6
Nonanol (C_9)	-4.4	-4.2	-4.8
Decanol (C_{10})	-4.7	-4.0	-5.0
Undecanol (C_{11})	-4.8	-4.4	-4.8
Dodecanol (C_{12})	-4.8	-4.5	-5.2
Tridecanol (C_{13})	-4.5	-4.4	-4.9
Tetradecanol (C_{14})	-4.6	-4.6	-5.2
Pentadecanol (C_{15})	-4.9	-4.3	-5.5
Isoniazid	-4.9	-5.2	-5.3
Triclosan	-6.4	-6.7	-7.0

Furthermore, observation of the binding energy of each alcoholic compounds in Table 2 suggests that the longer C-atoms chain in the alcohol resulted in the higher binding energy (in more negative values of ΔG) between the ligand and receptor.For instance,the binding energy for pentadecanol-PanK was ΔG = -5.5 kcal/mol, for pentandecanol-InhA ΔG = -4.9 kcal/mol, and for pentadecanol-MabA ΔG = -4.3 kcal/mol.

Compared with isoniazid, the alcoholic compoundsC_{10}-C_{15} exhibited a similar ability as an inhibitor of InhA, MabA, and PanK as isoniazid. The binding was -4.9 kcal/mol, -4.9 kcal/mol, and -5.3 kcal/mol, respectively. In contrast to the binding energy of triclosan as an inhibitor, for three receptors were relatively stronger than the alcoholic compounds. The

DOI: http://dx.doi.org/10.14203/ann.bogor.2018.v22.n2.101-115

affinity energy of triclosan with InhA, MabA, and PanK were -6.4 kcal/mol, -6.7 kcal/mol, and -7.0 kcal/mol respectively. Based on the binding energy from isoniazid and triclosan, the type of alcohol (C_{10}-C_{15}) has the ability for the inhibition of InhA, MabA, and PanK.

Ligand-receptor interaction.

Regarding the Gibbs free energy (ΔG) data in Table 2, pentadecanol represented the more potent ligand than the other alcoholic compounds in inhibiting InhA and PanK with ΔG = -4.9 kcal/mol and -5.5 kcal/mol, respectively, whereas tetradecanol was the most potent ligand in the inhibition of MabA (ΔG = -4.6 kcal/mol).

a. Pentadecanol-InhA

Among the 15 alcoholic compounds docked with InhA, pentadecanol was found to have a more negative Gibbs free energy (ΔG) than other ligands (ΔG = -4.9 kcal/mol) (Table 2).

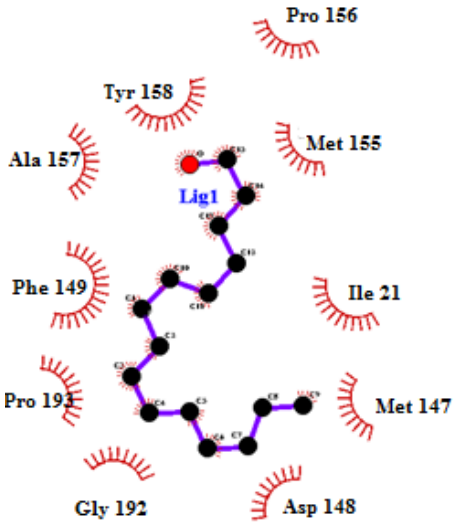

Figure 1. The interaction between pentadecanol (C_{15}) toward InhA residues with Gibbs free energy (ΔG) is -4.9 kcal/mol. The black dots represent 15 C- atoms of pentadecanol and the red one is the O-atom of the hydroxyl group at C_{15}. The red signs are the hydrophobic residues around the pentadecanol. Two of the hydrophobic residues Met155 and Phe 149around the pentadecanol form the binding site of InhA (Table 1).

Pentadecanol is an alcoholic compound with 15C-atoms and created hydrophobic interactions with InhA residues Met155, Ile21, Met147, Asp148, Gly192, Pro193, Phe149, Ala157, Tyr158 and Pro 156. No hydrogen bond was found in the interaction between pentadecanol and InhA. The orientation and interaction of pentadecanol while docked with InhAis depicted in Fig. 1 and 2.

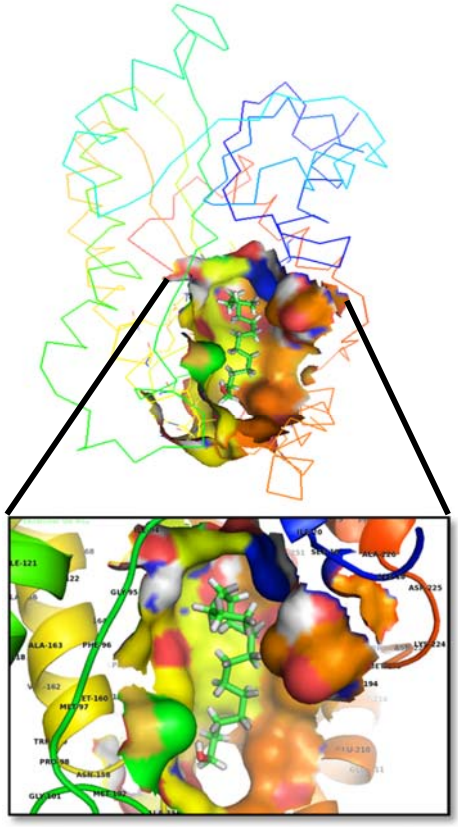

Figure 2. The three-dimensional interaction between pentadecanol (C_{15}) towards the InhA receptor. The top picture is the visualization of the position and orientation of pentadecanol with respect to the whole InhA. The bottom picture reveals the interaction of pentadecanol with its putative binding site in InhA.

b. Pentadecanol-PanK

Pentadecanol was the most potent ligand (ΔG: -5.5 kcal/mol) towards PanK compared to 14 other alcoholic compounds (Table 2). The binding energy was affected by the pentadecanol orientation while docked with PanK (Fig. 4)

Pentadecanol in PanK created interactions with PanK hydrophobic residues, *i.e.*, Phe254, Phe 239, Arg 238, Met 242, Lys147, Tyr235, Tyr182, Tyr 257, Ile 272, Phe 247 (Fig. 4). Further, there was a hydrogen bond between the hydroxyl group at C_{15} of pentadecanol with carbonyl

DOI: http://dx.doi.org/10.14203/ann.bogor.2018.v22.n2.101-115

O-atom of Lys147 residue in PanK. The length of the hydrogen bond was 3.04 Å

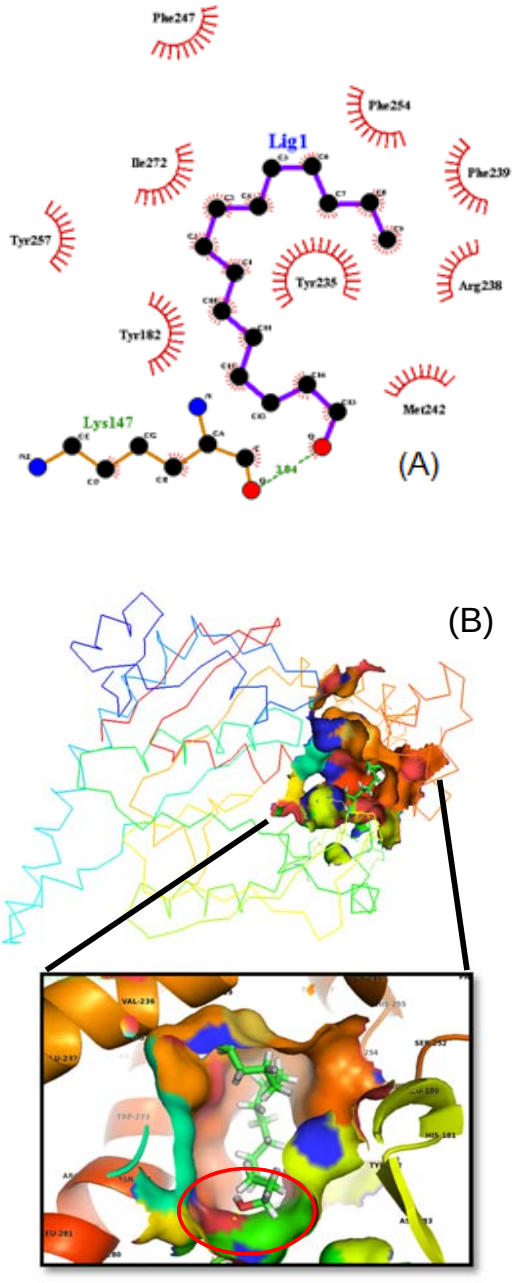

Figure 3. (A) The interaction between pentadecanol (C_{15}) with PanK residues with a Gibbs free energy (ΔG) of -5.5 kcal/mol. The black dots represent 15 C-atoms of pentadecanol, and the red one is the O atom of the hydroxyl group at C_{15}. The symbols in red are the hydrophobic residues around the pentadecanol. The hydrogen bond occurs between the hydroxyl O-atom at C_{15} of pentadecanol with the carbonyl O-atom of Lys147. The dotted line is the length of the hydrogen bond. (B) The interaction between pentadecanol (C_{15}) with PanK as the receptor. The top picture shows the position and orientation of pentadecanol with respect tothe whole PanK. The bottompicturedisplaysthe interaction of pentadecanol with its putative binding site in PanK.The red stick in the ligand structure is the hydroxyl O-atom while interacting with the carbonyl O-atom of Lys147 (red circle).

c. Tetradecanol-MabA

Tetradecanol (C_{14}) was the most potent inhibitor for MabA among the alcohols used in this study with the Gibbs free energy (ΔG) of -4.6 kcal/mol for the binding with MabA.

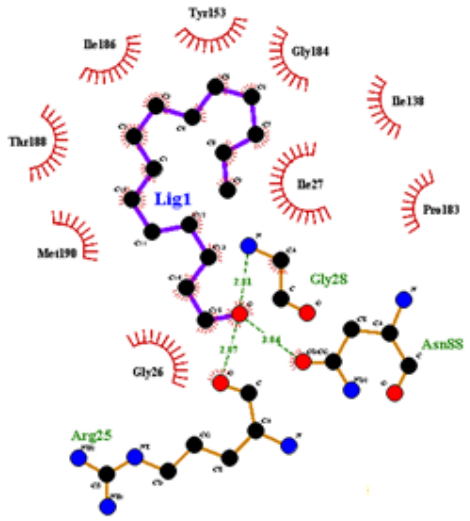

Figure 4. The interaction between tetradecanol (C_{14}) toward MabA residues with Gibbs free energy (ΔG) of -4.6 kcal/mol. The black dots represent 14 C- atoms of tetradecanol and the red one is the O-atom of the hydroxyl group in C_{14}. The symbols in red are the hydrophobic residues around tetradecanol. Residues Arg25, Gly28, and Asn88formhydrogen bond side-chain contacts with O-atom at C_{14} of tetradecanol. The carbonyl O-atom of Arg25makes a hydrogen bond with the length of 2.87Å. From the interaction map, there is also a hydrogen bond with a length of 2.81 Å with the peptidyl N-atom in Gly28 and a hydrogen bond with a length 3.04 Åwithcarbamoyl O-atom of Asn88.

The hydrophobic residues from MabA around the tetradecanol included Tyr153, Gly184, Ile138, Ile27, Pro183, Gly28, Asn88, Arg25, Gly26, Met190, Thr188,

Annales Bogorienses Vol. 22, No. 2, 2018
DOI: http://dx.doi.org/10.14203/ann.bogor.2018.v22.n2.101-115

Ile186. Some of the residues around the tetradecanol were binding site residues, *i.e.*, Tyr153, Asn88, and Ile138

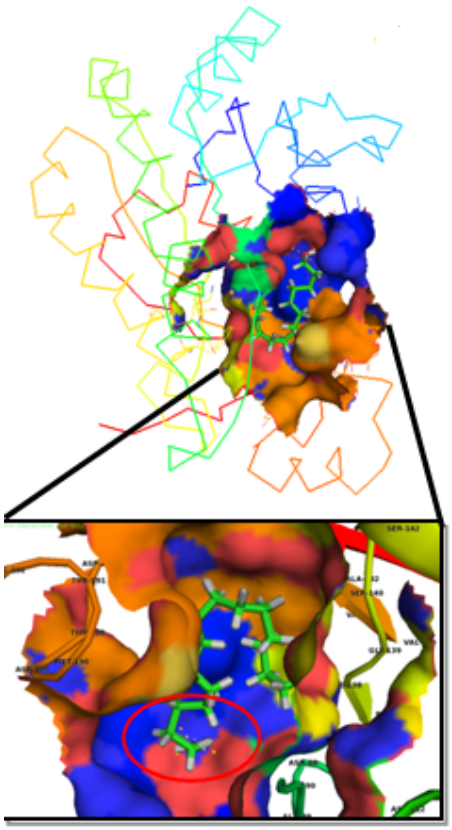

Figure 5. The interaction between tetradecanol (C_{14}) toward MabA. The orientation and interaction of tetradecanol with the residues at the putative binding site of MabAare shown (see also Table 1). The red circles indicate the location of three hydrogen bonds (see also Fig. 4).

All of the potential ligands were bound in the binding site of each receptor wherein the residues in the binding site are the best residues for docking the ligand (Fig. 1-5). Furthermore, the ligand interacted with other residues in each receptor which influenced the configuration of energy in the receptor-ligand complex (Table 2). However, we needed to further investigate the stability of receptor-ligand binding complex by using molecular dynamics analysis.

Discussion

The virtual screening potency of alcoholic compounds.

Virtual screening is computational biological screening to discover new ligands on the basis of biological structures (Kumar *et al.*, 2014). Hence, we performed virtual screening analysis to investigate the suitability of alcoholic compounds (C_1-C_{15}) as mycobactericidal agents.

Alcoholic compounds have been utilized as research objects to develop a disinfectant or antiseptic agent. The study from Kubo *et al*. (1995) on the use of the alcoholic and common naturally occurring alcohols as antimicrobial agents concluded that long-chain alcohols were effective against all the Gram-positive bacteria, yeasts and molds tested, but not as much against Gram-negative bacteria. Specifically, dodecanol has a maximum activity against *S.mutans*, therefore should be admissible for oral care products as anticavity agents. Accordingly, it was suggested that modest and definable differences in a compound could lead to an antimycobacterial activity depending on a balance between the hydrophilic and hydrophobic portion of the molecule (Rugutt and Rugutt, 2012). Mukherjee K *et al*. (2013) claimed that alcohols with more than ten carbon atoms have a drastic reduction in activity starting from n-hexane to n-decane which showed no inhibitory action against *M. smegmatis*. The result showed the increase in lipophilicity related with antimycobacterial activity.

InhA is composed of 269 amino acids and consisting of seven β-sheet strands and eight α-helix (Dessen A *et al*., 1995). InhA has two binding sites, one being the place for coenzyme NADH and the other as the binding site of the substrate (2-trans-dodecenoyl-CoA). There are three loops which are essential components of the substrate-binding site, the substrate-binding loop (loop 1), loop 2 and loop 3. (Pauli *et al*., 2013) (Fig. 6). In searching for the inhibitor to InhA, molecules that bind to NADH binding site should be avoided, since NADH is also a coenzyme for many other metabolic enzymes.

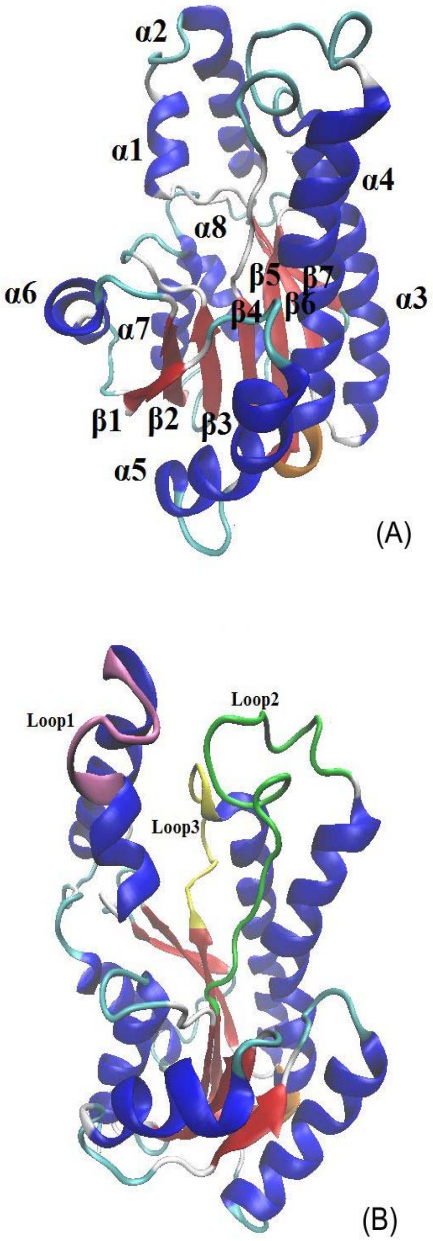

Figure 6. (A) The InhA structure, there are eight α-helix (blue) and seven β-sheet (maroon), some of the α-helix and β-sheet extend over the binding site of NADH. (B) The location of loop 1 (purple) comprising residuesGly204 to Glu209; loop 2 (green) which is composed of Ser94 to Pro107; loop 3 (yellow) is composed of Phe149 toTyr158. The loops were the location of the binding site of the substrate.

Pentadecanol docked with InhA showed hydrophobic interactions on the part of the binding site of the substrate (Fig. 1 and Fig. 2). The majority of hydrophobic residues that interact with the pentadecanoate on loop 2 (Fig.6B), *i.e.*, Phe149, Met155, Pro156, Ala157, and Tyr158. The interaction of pentadecanol with other hydrophobic residue was found on the α6 structure (Ile21), on the β5 structure (Met147 and Asp148), while the other are two residuesGly192 and Pro193located on the loop between α1 and β6 (Fig. 2 and Fig. 6A). The Tyr158 residue which is essential in the catalytic process of InhA is an electrophilic catalyst, which can transfer hydrogen bonding at the InhA with the substrate. Also, mutation of Ser94 on InhA to Ala94 is one of the factors of resistance of Mycobacterium to isoniazid (Rozwarski *et al*., 1999; Shilpi *et al*., 2015)

Pentadecanol has fifteen rotatable bonds, thereby giving effect on the orientation of the pentadecanol on the binding site of InhA. Pentadecanol affinity with InhA was-4.9 kcal/mol which was the best affinity among the 15ligands (Table 2). No hydrogen bond was found in the interaction between pentadecanol with InhA. The interaction of InhA and pentadecanol could also is enhanced by the existence of other chemical interactions that enable higher affinity. The possible chemical interaction is van der Waals interactions, which have an energy of about 0.4 to 40 kJ/mol. Under optimal circumstances, van der Waals interactions can achieve bonding energies as high as 40 kJ/mol (Pollard *et al*., 2016). Hydrophobic interactions with residues around the ligand affect ligand-receptor stability. Isoniazid and pentadecanol have the same affinity (-4.9 kcal/mol), but the interactions are different (Fig. 1 and Fig. 7). Pentadecanol has a flexible structure compared to isoniazid with an only one rotatable bond that makes orientation in binding with the InhA has betters stability and affinity. Triclosan has a superior affinity because it can be precisely bound at the binding site of InhA in substrate binding site or NADH binding site. The affinity of triclosan is also influenced by the Tyr158 which is a catalytic residue of InhA and surrounded by hydrophobic residues of the InhA binding site.

Annales Bogorienses Vol. 22, No. 2, 2018
DOI: http://dx.doi.org/10.14203/ann.bogor.2018.v22.n2.101-115

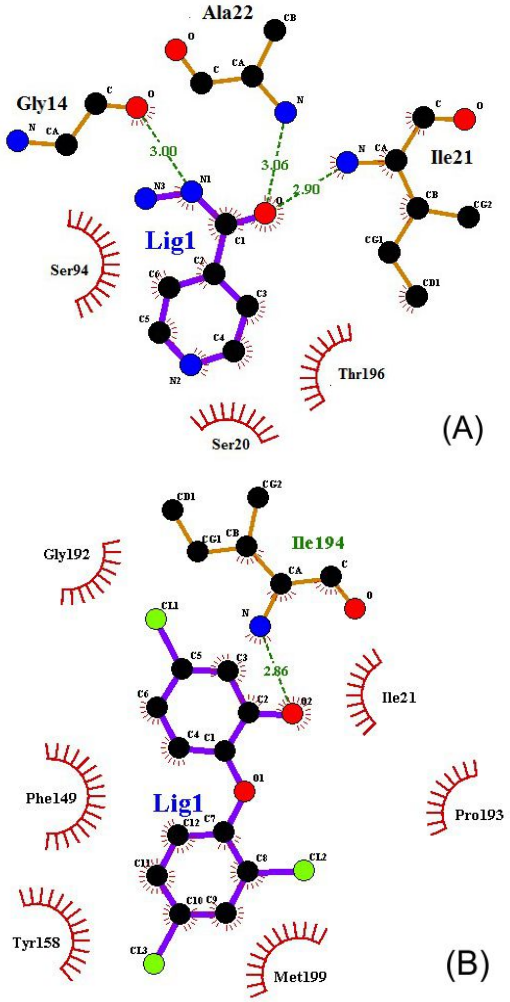

Figure 7. (A) The interaction between isoniazid and residues in InhA. There are three hydrogen bonds(indicated by dashed lines) with residues Ala22, Ile21, and Gly14, respectively. The hydrophobic interactions occur with Ser20, Thr196, and Ser94. The affinity between InhA and isoniazid was -4.9 kcal/mol (Table 2). (B) The two-dimensional structure of the interaction between triclosan and residues in InhA. There is one hydrogen bond between triclosan and Ile194 with a length of 2.86 Å. The affinity between InhA and triclosan is-6.4 kcal/mol.

The Gibbs free energy (Table 2) between tetradecane and MabA was-4.6 kJ/mol, suggesting that tetradecanol was the most potent inhibitor compared to 14 other alcoholic compounds.As the comparison, isoniazid and triclosan represent ligands with a higher affinity than all alcoholic compounds. MabA consists of 247 amino acids, forming6 α-helix and 7 β-sheet (Fig. 8A). The binding site of MabA is formed predominantly by the loop structures (Table 2 and Fig. 8B). The MabA residues around tetradecanol are Tyr153, Asn88, and Ile138 (Fig. 4).

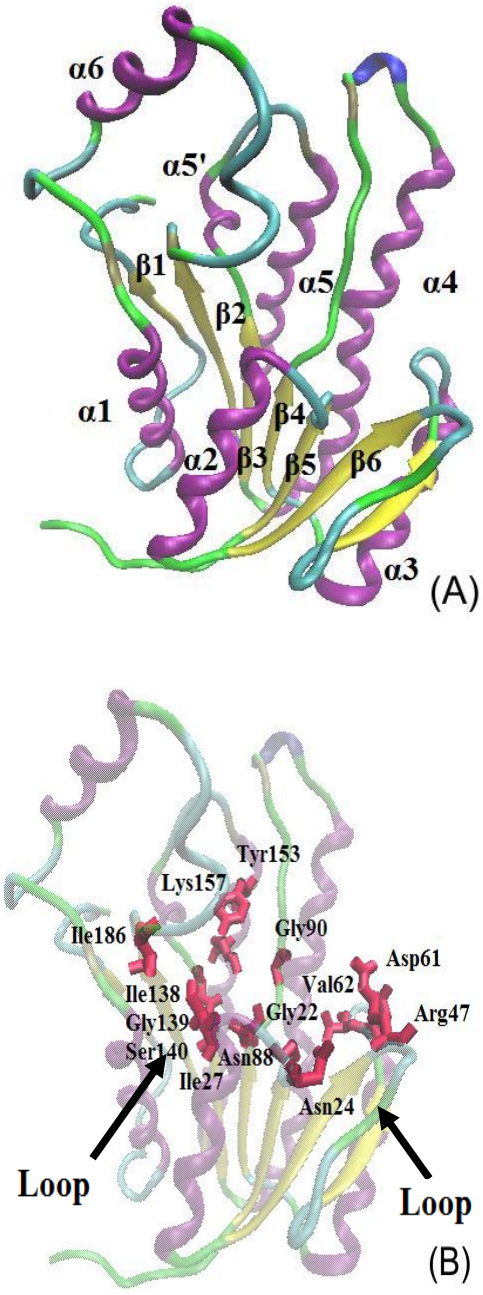

DOI: http://dx.doi.org/10.14203/ann.bogor.2018.v22.n2.101-115

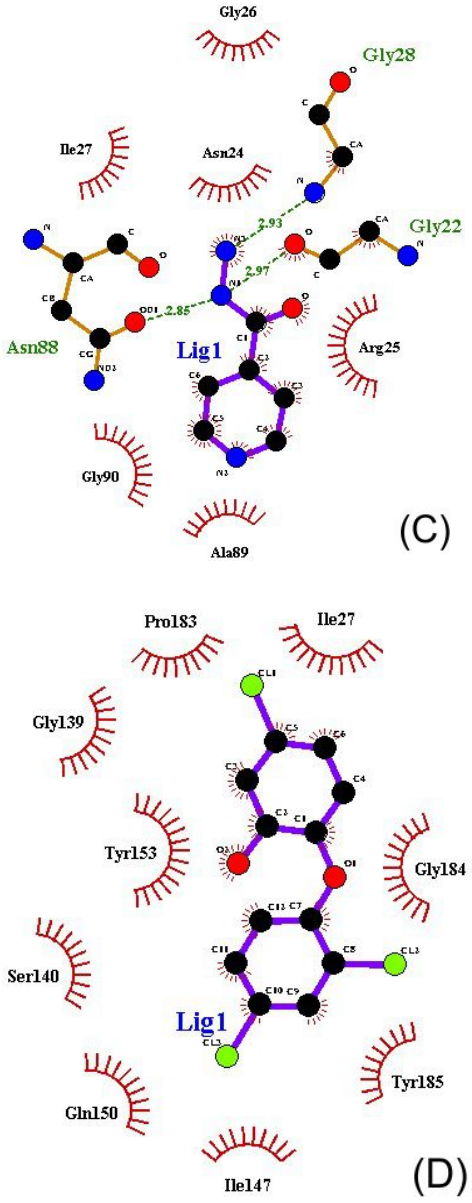

Figure 8. (A) the structure of MabA, α-helix structure (purple) and β-sheet structure (yellow) (B) binding site of MabA, residues in binding site (red) are dominant in the loop structure. (C) Interaction of isoniazid-MabA, there are three hydrogen bonds; Natom with O atom on Gly22 with length 2.97 Ā and with O atom with N atom Asn88 with length 2.85 Ā, N atom with N atom on Gly28 with length 2.93 Ā. The Gibbs free energy used is-5.2 kcal/mol (D) No hydrogen bond was found between interaction for triclosan with MabA with energy used was-6.7 kcal/mol.

Two loop structures of MabA became a dominant area in the binding of substrate. (Fig. 8B). The enzyme MabA represents a potential target in anti-mycobacterial drug design (Quemard *et al*. ,2006). Tetradecanol showed potential as an inhibitor of MabA, visible from the interaction at the binding site of MabA including with Tyr 153. Three residues of MabA, *i.e*., Ser140, Lys157, and Tyr153 (the catalytic triad) play a role in the binding of the substrate. The Tyr153 residue is core residue in the acid-base catalyst of MabA (Kavanagh *et al*., 2008; Shilpi *et al*., 2015). Some of the mutations important for the stability of the MabA have been reported including Ser140mutation that caused a decrease in the enzymatic activity of MabA (Rosado *et al*., 2012). In addition, mutations of Gly139 to Ala 139 (residues for the binding of cofactor NADPH) lead to inactivation of enzymes and the catalytic triad has a changed conformation (Poncet-Mantange *et al*., 2007; Rosado *et al*., 2012; Shilpi *et al*., 2015). Fig. 8D reveals that triclosan interacts with two residues from the catalytic triad of MabA (Ser140 and Tyr153), this allows a lower Gibbs free energy (ΔG) for triclosan-MabA complex than with other ligands.

Among the three receptors examined in this study, PanK was the best receptor interacting with all inhibitors (Table 2). CoA supported PanK biosynthetic pathway as a cofactor for catalysis processes (Begley *et al*., 2001) Pentadecanol interacts with PanK with the Gibbs free energy (ΔG) of-5.5 kcal/mol, which was higher than the affinity of InhA andMabA towards pentadecanol(-4.9 kcal/mol and-4.3 kcal/mol respectively). Fig. 9A shows the secondary structure PanK and the binding site residues,*i.e*., Gly97, Ser98, Val99, Ala100, Val101, Gly102, Lys103, Ser104. The residues are on the loop structure (p-Loop) which is the location of the Pank's substrate binding site (Chetnani *et al*., 2010). The structure of the p-loop serves for binding of ATP during the catalysis process (Shilpi *et al*., 2015). Pentadecanol interacts with some hydrophobic PanK residues (Fig. 3A). There are three residues; Tyr235, Met242, and Arg238 which are located around the p-loop (Fig. 9A). If compared to the location for the binding of triclosan to PanK, the binding location tends to be similar for the binding of pentadecanoic PanK. One hydrogen bonds in pentadecanol–PanK complex was between the hydroxyl O-atom of pentadecanol with the carbonyl O-atom of Lys147. As a comparison, triclosan with a Gibbs free energy (ΔG) of-7.0 kcal/mol also

DOI: http://dx.doi.org/10.14203/ann.bogor.2018.v22.n2.101-115

interacts by a hydrogen bond with His179 in the PanK binding site. Additionally, the interaction with His179 was further stabilized by a hydrogen bond between His179 and Asp129(Fig. 9B).

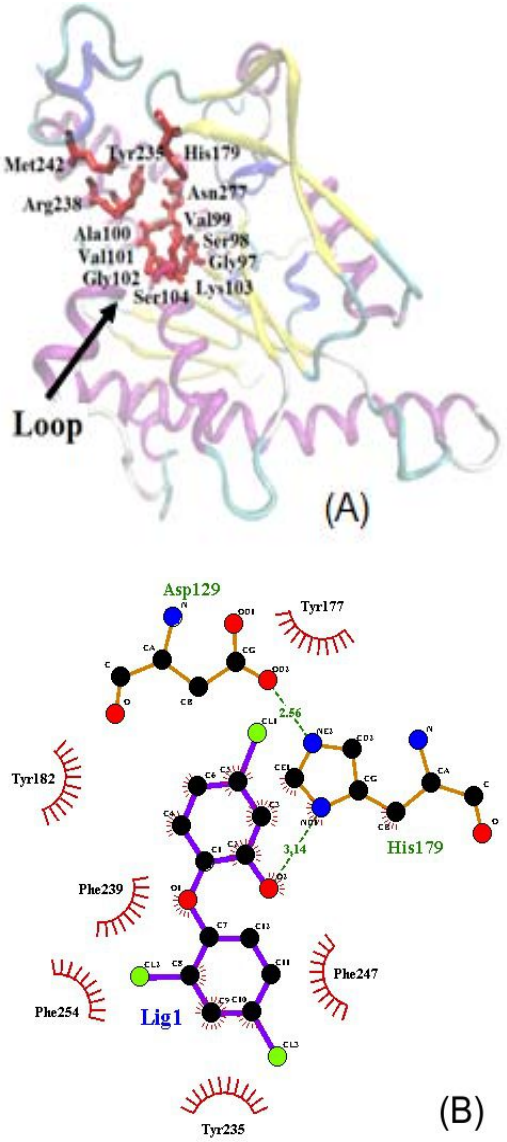

Figure 9. (A) the residues (red) in the PanK binding site, the arrow shows the p-Loop (B) the interaction between the hydrophobic residues ofPanK with triclosan. There are two hydrogen bonds indicated by a dotted line.

Molecular dynamics simulations.

The most potent ligand-receptor complex based on molecular docking result was further subjected to all-atom MD simulation to investigate the stability of ligand-receptor complex in the solvent. We selected the Pentadecanol–PanK complex based on the lowest binding free energy according to Table 2. Fig.10 shows the time evolution of the root mean square deviation (RMSD) value which was obtained from MD simulation of PanK protein in complex with pentadecanol. The RMSD value of the complex is not significantly fluctuated during the simulation and in equilibrium within the time range. Then, we used the snapshot at 5000 ps to estimate the binding affinity of pentadecanol–PanK complex by using docking simulation.

Re-docking of pentadecanol – PanK for 5ns.

Re-docking aimed to observe the stability of protein-ligand interactions from molecular dynamics (MD) result. In addition, the re-docking conducted to evaluate the orientation and flexibility of the protein and ligand interaction after molecular dynamics simulation.

In this study, we also carried out re-docking between pentadecanol and PanK structure from MD result. The PanK structure that changes after MD at 300 K and 1 atm for 5 ns (PanK5ns) (Fig. 11B and 11C). The analysis of the re-docking indicated that PanK 5ns remained stable interacting with pentadecanol on the binding site of p-Loop with Gibbs free energy of ΔG = -5.5 kcal/mol (Fig. 11A), which was

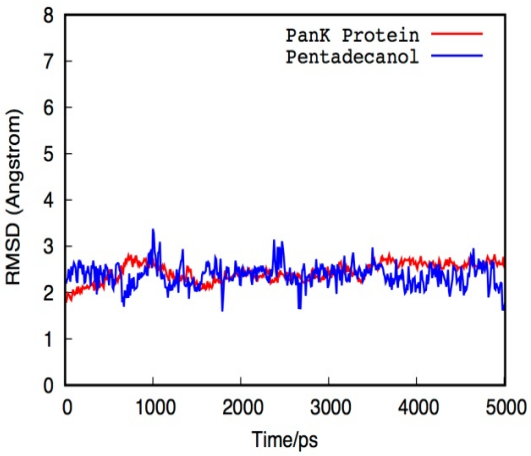

Figure 10. The RMSD values of Pentadecanol – PanK complex during the simulation for 5000 ps. The blue and red line demonstrated the stability of pentadecanol and PanK, respectively. The PanK and pentadecanol exhibited stable structure from 0 to 3000 ps which suggested a non-significant fluctuation during the simulation.

DOI: http://dx.doi.org/10.14203/ann.bogor.2018.v22.n2.101-115

similar with ΔG of initial PanK (before MD) of-5.5kcal/mol. The hydrophobic area of pentadecanol interacting with PanK5ns was similar with pentadecanol interaction with PanK (dominant in the p-Loop area) (Fig. 3A and 11A)

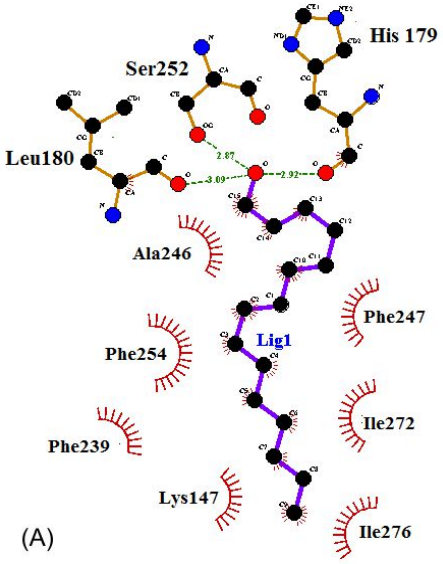

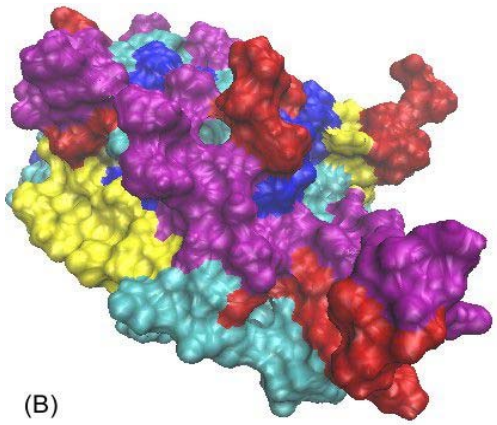

Figure 11. (A) the interaction between the pentadecanol with PanK2ns. A slight change in residue interactions between the pentadecanol – PanK2ns and pentadecanol PanK (Figure 3A). Three hydrogen bond interaction in O atom with O atom in His179, Leu 180, and Ser252. (B) Three-dimensional of PanK before to MD simulation (D) three-dimensional PanK after MD on 5n at 300 k and 1 atm (PanK5ns). The difference in color showed the secondary

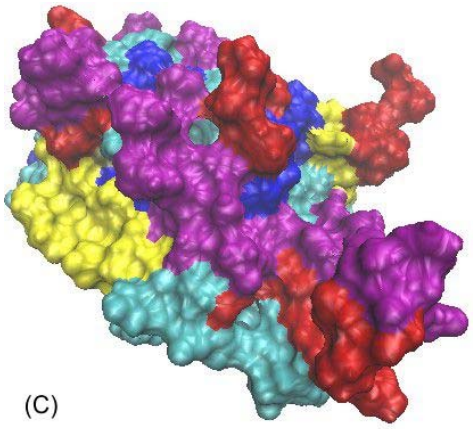

structure: α-helix (purple), a β-sheet (yellow), loop (cyan), 3-10 helix (blue), coil (red)

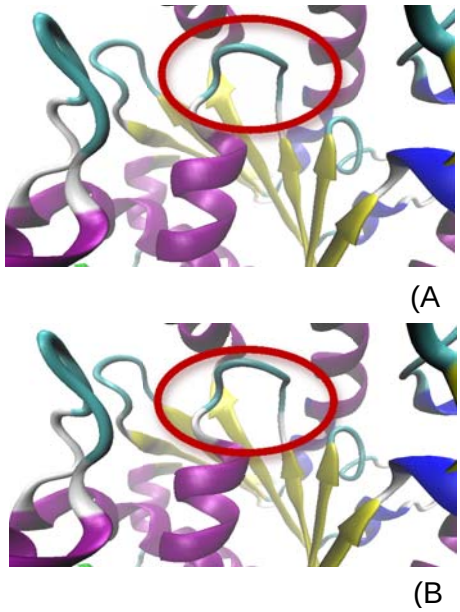

Figure 12. (A) p-Loop condition before molecular dynamic simulation. (B) p-Loop condition after molecular dynamic simulation.

Fig. 12A and 12B represent the alteration in PanK secondary structure after molecular dynamics simulation for5 ns. The PanK structure was demonstrated a stable condition after MD simulation. However, the binding residues for pentadecanol exhibited a small shift in the p-Loop area. Interestingly, the binding energy before and after molecular dynamics was of the same values.

In conclusion, the appropriate disinfectant mycobactericidal influenced by some of the factors; 1) receptor as the target inhibition process, 2) the ligand as an inhibitor, 3) the stability of interaction between the receptor and

Annales Bogorienses Vol. 22, No. 2, 2018
DOI: http://dx.doi.org/10.14203/ann.bogor.2018.v22.n2.101-115

ligand. Based on the molecular docking and molecular dynamics simulation, the alcoholic compounds C_{10}-C_{15} have potency as mycobactericidal agents. Pentadecanol is more appropriate as a mycobactericidal agent because of its affinity towards InhA, PanK, and MabA.In addition, PanK structure was relatively stable after molecular dynamics in 5 ns. The future research will focus on the unfolding mechanism of PanK structure. Pentadecanol-PanK can be used as a reference to develop a mycobactericidal agent with a specific target receptor in *Mycobacterium.*

Acknowledgments

The authors would like to thank as Eka Arismayanti for supporting docking simulation for some of the ligand-receptor.

References

Alonso, H., Bliznyuk, A. A., & Gready, J. E. (2006). Combining docking and molecular dynamic simulations in drug design.*Medicinal research reviews*, *26*(5), 531-568.

Banerjee, A., Dubnau, E., Quemard, A., Balasubramanian, V., Um, K. S., Wilson, T., ... & Jacobs, W. R. (1994). inhA, a gene encoding a target for isoniazid and ethionamide in Mycobacterium tuberculosis. *Science*, *263*(5144), 227-230.

Begley, T. P., Kinsland, C., & Strauss, E. (2001). The biosynthesis of coenzyme A in bacteria. *Vitamins & Hormones*, *61*, 157-171.

Bloom, B. R., & Murray, C. J. (1992). Tuberculosis: commentary on a reemergent killer. *Science*, *257*(5073), 1055-1064.

Brennan, P. J. (2003). Structure, function, and biogenesis of the cell wall of *Mycobacterium tuberculosis. Tuberculosis*, *83*(1-3), 91-97.

Christopher, D. J., Daley, P., Armstrong, L., James, P., Gupta, R., Premkumar, B., ... & Dendukuri, N. (2010). Tuberculosis infection among young nursing trainees in South India. *PLoS One*, *5*(4), e10408.

Curtis, A. B., Ridzon, R., Novick, L. F., Driscoll, J., Blair, D., Oxtoby, M., McGarry, M., Hiscox,B., Faulkner,C., Taber,H., Onorato,I.M., & Valway, S. (2000). Analysis of *Mycobacterium tuberculosis* transmission patterns in a homeless shelter outbreak. *The International Journal of Tuberculosis and Lung Disease*, *4*(4), 308-313.

Dauendorffer, J. N., Laurain, C., Weber, M., & Dailloux, M. (1999). Effect of methodology on the tuberculocidal activity of a glutaraldehyde-based disinfectant. *Applied and environmental microbiology*, *65*(9), 4239-4240.

Dessen, A., Quemard, A., Blanchard, J. S., Jacobs, W. R., & Sacchettini, J. C. (1995). Crystal structure and function of the isoniazid target of *Mycobacterium tuberculosis*. *Science*, *267*(5204), 1638-1641.

Ehrenkranz, N. J., & Kicklighter, J. L. (1972). Tuberculosis outbreak in a general hospital: evidence for airborne spread of infection. *Annals of Internal Medicine*, *77*(3), 377-382.

Escombe, A. R., Huaroto, L., Ticona, E., Burgos, M., Sanchez, I., Carrasco, L., Farfan E., Flores, F & Moore, D. A. J. (2010). Tuberculosis transmission risk and infection control in a hospital emergency department in Lima, Peru. *The international journal of tuberculosis and lung disease*, *14*(9), 1120-1126.

Falkinham III, J.O., Macri, R.V., Maisuria, B.B., Actis, M.L., Sugandhi, E.W., Williams, A.A., Snyder, A.V., Jackson, F.R., Poppe, M.A., Chen, L. and Ganesh, K., (2012). Antibacterial activities of dendritic amphiphiles against nontuberculous mycobacteria. *Tuberculosis*, *92*(2), 173-181–181

Hatipoglu, M., Mutluoglu, M., Turhan, V., Uzun, G., Lipsky, B. A., Sevim, E., ... & Ay, H. (2016). Causative pathogens and antibiotic resistance in diabetic foot infections: A prospective multi-center study. *Journal of Diabetes and its Complications*, *30*(5), 910-916.

Hauer, B., Fiebig, L., Brodhun, B., & Haas, W. (2012). Tuberculosis surveillance and control in Germany—An application of the Berlin Declaration Monitoring and Evaluation Framework. *European Journal of Microbiology and Immunology*, *2*(4), 287-291.

Jackowski, S., & Rock, C. O. (1981). Regulation of coenzyme A biosynthesis. *Journal of Bacteriology*, *148*(3), 926-932.

Jackson, M., McNeil, M. R., & Brennan, P. J. (2013). Progress in targeting cell envelope biogenesis in *Mycobacterium tuberculosis*. *Future Microbiology*, *8*(7), 855-875.

Kabelitz, N., Santos, P. M., & Heipieper, H. J. (2003). Effect of aliphatic alcohols on growth and degree of saturation of membrane lipids in *Acinetobacter calcoaceticus*. *FEMS microbiology letters*, *220*(2), 223-227.

Kapetanovic, I. M. (2008). Computer-aided drug discovery and development (CADDD): in silico-chemico-biological approach. *Chemico-biological interactions*, *171*(2), 165-176.

Kato, S., & Mori, T. (2016). Advancing tuberculosis screening in Japan: Historical considerations and the way forward. *Respiratory investigation*, *54*(6), 484.

Kavanagh, K. L., Jörnvall, H., Persson, B., & Oppermann, U. (2008). Medium-and short-chain dehydrogenase/reductase gene and protein

families. *Cellular and Molecular Life Sciences*, *65*(24), 3895.

Kubo, I., Muroi, H., & Kubo, A. (1995). Structural functions of antimicrobial long-chain alcohols and phenols. *Bioorganic & medicinal chemistry*, *3*(7), 873-880.

Kumar, A., Gupta, R., Verma, K., Iyer, K., Shanthi, V., & Ramanathan, K. (2014). Identification of Novel Hepatitis C virus NS3-4A protease inhibitors by virtual screening approach. *Journal of Microbial and Biochemical Technology*, *6*(4), 1-7.

Kunz, R., & Gundermann, K. O. (1982). Survival of *Mycobacterium tuberculosis* on surfaces at different air-humidities. *Zentralblatt fur Bakteriologie, Mikrobiologie und Hygiene. 1. Abt. Originale B, Hygiene*, *176*(2-3), 105.

Kuyinu, E. L., Narayanan, G., Nair, L. S., & Laurencin, C. T. (2016). Animal models of osteoarthritis: classification, update, and measurement of outcomes. *Journal of orthopedic surgery and research*, *11*(1), 19.

Larson, E. L., & 1994 APIC Guidelines Committee. (1995). APIC guidelines for handwashing and hand antisepsis in healthcare settings. *American journal of infection control*, *23*(4), 251-269.

Leonardi, R., Zhang, Y. M., Rock, C. O., & Jackowski, S. (2005). Coenzyme A: back in action. *Progress in lipid research*, *44*(2), 125-153.

Marrakchi, H., Lanéelle, G., & Quémard, A. (2000). InhA, a target of the antituberculous drug isoniazid, is involved in a mycobacterial fatty acid elongation system, FAS-II. *Microbiology*, *146*(2), 289-296.

Marrakchi, H., Zhang, Y. M., & Rock, C. O. (2002). Mechanistic diversity and regulation of Type II fatty acid synthesis. *Biochemical Society Transactions*. 30(6), 1050-1055.

Mohle-Boetani, J. C., Miguelino, V., Dewsnup, D. H., Desmond, E., Horowitz, E., Waterman, S. H., & Bick, J. (2002). Tuberculosis outbreak in a housing unit for human immunodeficiency virus-infected patients in a correctional facility: transmission risk factors and effective outbreak control. *Clinical infectious diseases*, *34*(5), 668-676.

Morton, H. E. (1983). Alcohols. *Disinfection, Sterilization and Preservation*. 3rd edition edited by S.S Block. Philadelphia, USA: Lea and Febiger

Mukherjee, K., Tribedi, P., Mukhopadhyay, B., & Sil, A. K. (2013). Antibacterial activity of long-chain fatty alcohols against mycobacteria. *FEMS microbiology letters*, *338*(2), 177-183.

OR Júnior, C., Le Hyaric, M., da Costa, C. F., Corrêa, T. A., Taveira, A. F., Araújo, D. P., & de Almeida, M. V. (2009). Preparation and antitubercular activity of lipophilic diamines and amino alcohols. *Memórias do Instituto Oswaldo Cruz*, *104*(5), 703-705.

Pauli, I., Dos Santos, R. N., Rostirolla, D. C., Martinelli, L. K., Ducati, R. G., Timmers, L. F., ... & Norberto de Souza, O. (2013). Discovery of new inhibitors of *Mycobacterium tuberculosis* InhA enzyme using virtual screening and a 3D-pharmacophore-based approach. *Journal of chemical information and modeling*, *53*(9), 2390-2401.

Pollard, T. D., Earnshaw, W. C., Lippincott-Schwartz, J., & Johnson, G. (2016). *Cell Biology E-Book.* 3rd edition. Philadelphia, USA – London, UE. Elsevier Health Sciences.

Poncet-Montange, G., Ducasse-Cabanot, S., Quemard, A., Labesse, G., & Cohen-Gonsaud, M. (2007). Lack of dynamics in the MabA active site kills the enzyme activity: practical consequences for drug-design studies. *Acta Crystallographica Section D: Biological Crystallography*, *63*(8), 923-925.c

Quemard, A., Labesse, G., Daffe, M., Marrakchi, H., Douguet, D., Cohen-Gonsaud, M., & Ducasse, S. (2006). *Use of the protein MabA (FabG1) of Mycobacterium tuberculosis for designing and screening antibiotics*. (U.S. Patent Application No: US20060035294A1).

Rock, C. O., Karim, M. A., Zhang, Y. M., & Jackowski, S. (2002). The murine pantothenate kinase (PanK) gene encodes two differentially regulated pantothenate kinase isozymes. *Gene*, *291*(1), 35-43.

Roe, D. R. & Cheatham, T. E. (2013) PTRAJ andCPPTRAJ: Software for processing and analysis of molecular dynamics trajectory data. *Journal of Chemical Theory and Computation***9,** 3084–3095

Rosado, L. A., Caceres, R. A., de Azevedo, W. F., Basso, L. A., & Santos, D. S. (2012). Role of Serine140 in the mode of action of Mycobacterium tuberculosis β-ketoacyl-ACP Reductase (MabA). *BMC research notes*, *5*(1), 526.

Rozwarski, D. A., Vilchèze, C., Sugantino, M., Bittman, R., & Sacchettini, J. C. (1999). Crystal structure of the Mycobacterium tuberculosis enoyl-ACP reductase, InhA, in complex with NAD+ and a C16 fatty acyl substrate. *Journal of Biological Chemistry*, *274*(22), 15582-15589.

Rugutt, J. K., & Rugutt, K. J. (2012). Antimycobacterial activity of steroids, long-chain alcohols,and lytic peptides. *Natural product research*, *26*(11), 1004-1011.

Rugutt, J. K., & Rugutt, K. J. (2012). Antimycobacterial activity of steroids, long-chain alcohols,and lytic peptides. *Natural product research*, *26*(11), 1004-1011.b

Russell, A. D. (1999). Bacterial resistance to disinfectants: present knowledge and future

DOI: http://dx.doi.org/10.14203/ann.bogor.2018.v22.n2.101-115

problems. *Journal of Hospital Infection*, *43*, S57-S68.

Rutala, W. A., & Weber, D. J. (1997). Water as a reservoir of nosocomial pathogens. *Infection Control & Hospital Epidemiology*, *18*(9), 609-616.

Salomon-Ferrer, R., Case, D. A. &Walker, R. C. (2013). An overview of the Amber biomolecular simulation package. *Wiley Interdisciplinary Reviews: Computational Molecular Science***3,** 198210.

Schneider, G., & Fechner, U. (2005). Computer-based de novo design of drug-like molecules. *Nature Reviews Drug Discovery*, *4*(8), 649.

Steart R.J., Tsang C.A., Pratt R.H., Price S.F., Langer A.J. (2018). Tuberculosis – United States, 2017. *Morbidity and Mortality Weekly Report, Centers for Disease Control and Prevention*, 67(11), 317-323.

Sykes, G. (1970). (Symposium on Bacterial Spores: Paper XII) The Sporicidal Properties of Chemical Disinfectants. *Journal of Applied Bacteriology*, *33*(1), 147-156.

Takayama, K., Wang, C., & Besra, G. S. (2005). Pathway to synthesis and processing of mycolic acids in *Mycobacterium tuberculosis*. *Clinical microbiology reviews*, *18*(1), 81-101.

Tambunan, U. S. F., Alkaff, A. H., Nasution, M. A. F., Parikesit, A. A., & Kerami, D. (2017). Screening of commercial cyclic peptide conjugated to HIV-1 Tat peptide as inhibitor of N-terminal heptad repeat glycoprotein-2 ectodomain Ebola virus through in silico analysis. *Journal of Molecular Graphics and Modelling*, *74*, 366-378.

Toms C., Stapledon R., Waring J., Douglas P. (2015). Tuberculosis notifications in Australia 2012 and 2013. *Annual Report National Tuberculosis Advisory*, 39(2),217.

Van Klingeren, B., & Pullen, W. (1987). Comparative testing of disinfectants against *Mycobacterium tuberculosis* and *Mycobacterium terrae* in a quantitative suspension test. *Journal of Hospital Infection*, *10*(3), 292-298.

Zhao, H., & Caflisch, A. (2015). Molecular dynamics in drug design. *European journal of medicinal chemistry*, *91*, 4-14.

Zhou, B., Westaway, S. K., Levinson, B., Johnson, M. A., Gitschier, J., & Hayflick, S. J. (2001). A novel pantothenate kinase gene (PanK) is defective in Hallervorden-Spatz syndrome. *Nature Genetics*

.